A&A 488, 279–286 (2008)
DOI: 10.1051/0004-6361:20079207

Astronomy & Astrophysics

Pulsating pre-MS stars in the young open cluster NGC 2264: V588 Monocerotis and V589 Monocerotis

T. Kallinger, K. Zwintz, and W. Weiss

Institute for Astronomy (IfA), University of Vienna, Türkenschanzstrasse 17, A-1180 Vienna, Austria
e-mail: kallinger@astro.univie.ac.at

Received 6 December 2007 / Accepted 18 June 2008

ABSTRACT

We report on the first high-accuracy, photometric multisite campaign to study the two, first-detected pulsating, pre-main sequence stars V588 Mon and V589 Mon in the direction of the young open cluster NGC 2264. We carried out the campaign from November 2002 to February 2003 with a photometric coverage of about 216 h at four observatories. A detailed frequency analysis results in well-populated eigenspectra, typical for δ Scuti type pulsation, with 16 and 20 significant frequencies in the V588 Mon and V589 Mon data, respectively. Using Strögrem *uvbyβ* photometry and spectroscopic observations as well as published Geneva and infrared photometry feasible fundamental parameters we deduced, placing both stars in the δ Scuti instability strip and giving strong evidence that both stars are members of NGC 2264 and are indeed in their pre-main sequence phase of evolution.

Key words. techniques: photometric – stars: pre-main sequence – Galaxy: open clusters and associations: individual: V588 Mon – stars: individual: V589 Mon – stars: oscillations – stars: fundamental parameters

1. Introduction

Intermediate mass stars (1.5 to ~5 $M_\odot$) cross the instability strip, in the middle of the Hertzsprung-Russell (HR-) diagram, during their gravitational contraction from birthline (Palla & Stahler 1993) toward the zero-age main sequence (ZAMS), where the gravitational contraction is balanced by nuclear fusion as the dominant energy source. Pre-main sequence (PMS) stars exhibit strong activity, such as large IR excesses and emission lines, as a consequence of their interaction with the circumstellar environment from which they were born and in which they are still embedded. This interaction can result in irregular variability. However, PMS stars spend about 5 to 10% of their total PMS contraction time in the instability region where they have an appropriate internal configuration to become pulsationally, unstable presumably driven by the κ (and/or γ) mechanism in the hydrogen and helium ionization zones.

On their way to the ZAMS, PMS stars intersect the evolutionary tracks of their evolved counterparts several times (e.g., Breger & Pamyatnykh 1998). At these intersections, PMS and post-MS stars have equal mass, luminosity, and temperature, hence similar envelope properties, and differ only in their internal structure. Whereas PMS stars possess a quite homogeneous inner structure, mostly defined by their gravitational collapse, the cores of post-ZAMS stars are modified by nuclear burning and the stars develop chemical inhomogeneities.

The positions of the currently known 36 pulsating PMS stars in the HR diagram were compared to those of the classical δ Scuti stars. The boundaries of the classical and the PMS instability regions seem to coincide, except for a lack of PMS pulsators in the "cool" corner of the classical instability strip (Zwintz 2008). For stars in the instability strip, stellar pulsation is driven by classical opacity mechanisms in the outer layers. Hence, it is reasonable to expect that PMS stars exhibit the same type of modes (with similar amplitudes) as their post-MS counterparts (see Suran et al. 2001, and references therein). However, the different internal structure is expressed in deviating frequency spectra. Whereas radial modes are mostly the same in PMS and post-MS stars (with equal mass and location in the HR-Diagram), low radial order non-radial mixed modes (gravity modes with pressure modes character in the outer regions) differ for the different evolutionary stages. These modes are very sensitive to the internal structure and can be used as an age discriminator. This was already proposed by Suran et al. (2001), but for the first time demonstrated by Guenther et al. (2007) where they have shown that the observed oscillations of the star NGC 6530 278 can only be fit by PMS models and not by post-MS models.

Breger (1972) found luminosity variations on timescales typical for δ Scuti type pulsation in the two stars V588 Mon (HD 261331, NGC 2264 2) and V589 Mon (HD 261446, NGC 2264 20) in the direction of the young open cluster NGC 2264. As the cluster is too young to include A to F stars having reached the main sequence, and both stars are presumably cluster members they are in their PMS phase and cannot be classical δ Scuti stars. Hence, they were classified as the first discovered PMS pulsators. Some 20 years later Kurtz & Marang (1995) discovered oscillations in the well-studied PMS field star HR 5999 followed by several detections of pulsation in known PMS field stars (e.g., Marconi et al. 2000) and members of young clusters (Zwintz et al. 2005; Zwintz & Weiss 2006).

Remarkably, Wolf (1924) was the first who discovered the variability of V588 Mon and V589 Mon by comparing photographic plates from different epochs. But he did not investigate the nature of the variability. Breger (1972) was the first who obtained photometric time series of A to F stars in NGC 2264. Since the data sets consist only of 3 nights distributed over a time-span of more than 2 years, he was only able to estimate

the periods for V588 Mon and V589 Mon to be roughly 2.6 and 2.9 h, respectively. But already these short snapshots clearly showed the multi-periodicity of the two stars.

Obviously, the crucial point for introducing them as pulsating PMS stars is their cluster membership. Up to now there is still no detailed study about their membership available. But Breger (1972) already concluded that both stars are most likely members. Both fit the HR-Diagram of the cluster. There is no radial velocity measurement available for V588 Mon, but V589 Mon has a radial velocity consistent with other cluster members (Strom et al. 1971). Furthermore, both stars have too short periods to be background and hence more luminous δ Scuti stars. Since A to F (sub-)giants are relatively rare, one is very unlikely to find two foreground field giants. We can add that the proper motion of both stars is in agreement with the cluster's average proper motion (Hog et al. 2000). And, we found prominent emission lines due to interstellar gas with similar radial velocities indicating that both stars are embedded in clouds of gas belonging to the cluster. Each of these arguments cannot prove cluster membership, but provide strong evidence that both stars are indeed members of NGC 2264.

Driven by Breger's discovery, Peña et al. (2001) reobserved the two stars in 1986 for 5 nights in the course of about 6 weeks. Using their Strömgen photometry, they give a distance for both stars of 530 ± 70 pc. Compared to the so far, best-known value for the distance of NGC 2264 of 760 ± 80 pc (see next section) both stars seem to be foreground stars. However, their distance uncertainty corresponds only to the formal error of the calibration based on the uncertainties of the observations. It has to be mentioned that Strömgen calibrations tend to become uncertain (or even fail) for non-main sequence stars and have in any case a nonnegligible error. Taking this into account, we interpret the Peña et al. (2001) result as a confirmation that both stars are at least close to NGC 2264.

We present multi-site, multi-color photometric time series as well as spectroscopic observations of V588 Mon and V589 Mon, a detailed frequency analysis, and a discussion of the fundamental parameters. As an outlook we announce that the high-precision observations of the Canadian micro-satellite MOST[1] and a detailed model analysis of both stars will be the topic of a follow-up paper.

2. The young open cluster NGC 2264

NGC 2264 ($\alpha_{2000} = 6^h41^m$, $\delta_{2000} = +9°53^m$) is a well studied large (>1° in diameter) HII region with active star formation, which is located in the direction of Monoceros about 30 pc above the galactic plane. It includes four astronomical objects as a single object (Cone Nebula, Christmas Tree Cluster, Snowflake Cluster, and the Fox Nebula).

The distance and age determination of NGC 2264 are very difficult because only stars of spectral type B (and hotter) are massive enough to have reached the ZAMS. Sung et al. (1997) concluded a distance modulus $(m - M)_V$ of 9.4 ± 0.25 mag, yielding a distance of 760 ± 80 pc, which is consistent with values found by others (e.g., Pérez et al. 1987). As the cluster is still an active star forming region there is no lower limit for the cluster age. However, Sung et al. (1997) determined the age of the cluster members to be in the range of 0.8 to 8 Myr, but with some stars being only 0.15 Myr old.

Since NGC 2264 is sufficiently nearby and fairly populous it is perhaps the best target for studying various phenomena, like the evolution of angular momentum during the PMS phase (Lamm et al. 2004) or the frequency of circumstellar disks surrounding PMS stars (Rebull et al. 2002). But all investigations have in common that they are focused on the inner (more populated) regions of the open cluster. Since V588 Mon and V589 Mon are located roughly 0.5° southwest of the cluster center at the edge of a dark nebula, both stars were not included in any of the cluster surveys so far.

3. Observations and data reduction

A 3-site photometric campaign of V588 Mon and V589 Mon was carried out from November 28 to December 15, 2002 with follow-up single site observations from December 28, 2002 to February 9, 2003. About 137.3 h of data were collected during the core part of the campaign and about 78.7 h during the follow-up observations resulting in a total observation time of ~216 h spanning roughly 74 days. The corresponding duty cycles are ~34% and ~12% for the core part of the campaign and the entire run, respectively.

The following telescopes were used:

1. The APT observations were obtained with the 75 cm Vienna Automatic Photoelectric Telescope, located at Washington Camp in Arizona, USA.
2. The OSN measurements were obtained with a four-channel photometer attached to the 90 cm telescope located at the Observatorio de Sierra Nevada in Granada, Spain.
3. The MKO observations were obtained with a 1 k × 1 k CCD mounted at the 22 inch telescope of the University of Hawaii located at the Mauna Kea Observatory in Hawaii, USA.
4. The SAAO measurements were made with the modular photometer attached to the 50 cm telescope at the South African Astronomical Observatory.

A summary of the observations is given in Table 1.

3.1. Photoelectric observations

The APT, OSN, and SAAO observations were obtained using standard photoelectric photometers with photomultiplier tubes as detectors. While the APT and SAAO observations were made through Johnson V and B filters using single-channel photometers, the OSN measurements were made simultaneously through Strömgren u, v, b, y filters using a multi-channel photometer. A standard four-star technique in which the measurements of the 2 program stars were alternated with 2 comparison stars was applied to monitor instrumental stability and atmospheric extinction. We used HD 47554 (V = 7.86 mag; F2 V) and HD 261355 (V = 8.23 mag; F5) as comparison stars . All data were corrected for the sky background monitored in 4 dedicated fields.

3.2. CCD observations

The MKO observations were carried out for 13 nights, using a 1 k × 1 k CCD detector with a scale of 0.53/pixel (field-of-view of ~9′ × 9′) and a broadband filter very similar to Johnson V. The integration time was typically 12 s with a sampling time of 1 min. Science frames were corrected for bias, dark and flat field within the reduction software Podex developed by

[1] The MOST (*Microvariability & Oscillations of STars*) satellite a Canadian Space Agency mission jointly operated by Dynacon, Inc., the University of Toronto Institute of Aerospace Studies, and the University of British Columbia, with assistance from the University of Vienna, Austria.

Table 1. Summary of observations.

observatory	start date end date	nights	length [h]	data points	filter
APT	11/28/02 12/15/02	8	53.6	173	B, V
OSN	12/02/02 12/15/02	7	43.8	314	u, v, b, y
MKO	11/27/02 12/10/02	13	56.6	3250	V
SAAO	12/28/02 02/09/03	24	78.7	198	B, V
total		52	~216	3935	

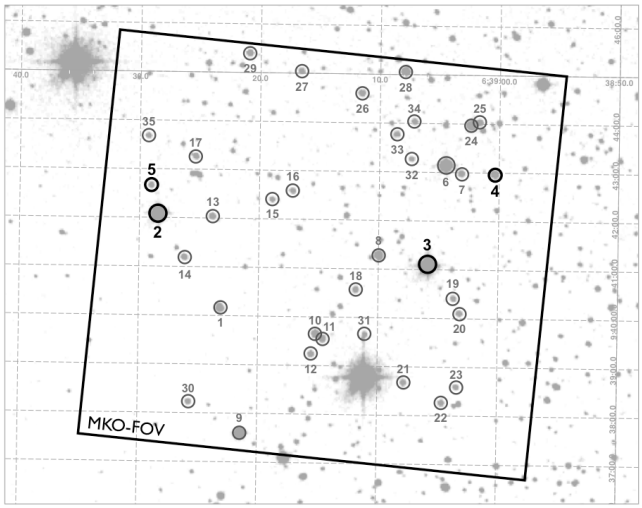

Fig. 1. MKO field-of-view ($9' \times 9'$). Circles indicate stars used for photometry. Bold labeled stars are found to be variable where 2 and 3 correspond to V588 Mon and V589 Mon, respectively.

Kallinger (2005). Podex uses a modified aperture photometry algorithm, optimized for crowded fields, for extracting photometric signal from CCD time series. It extracts time series for all selected stars and computes an average light curve from arbitrarily selected stars used as a comparison light curve for differential photometry. The advantage of Podex is an easy to use graphical interface simplifying the identification of variable stars to discard them from the computation of the comparison light curve. In total, the photometric signal of 34 stars in a V magnitude range of ~9.7–16 was extracted. Beside, the two known pulsators V588 Mon and V589 Mon, two additional stars were found to be variable. Both are most likely eclipsing binaries (see Sect. 7). Figure 1 shows the observed field where all analyzed stars are labeled. The 4 variable stars have bold numbers where 2 and 3 correspond to V588 Mon and V589 Mon, respectively.

3.3. Combining the data

Nightly means were subtracted from all reduced data to correct for zero-point shifts and intrinsic long-term trends. The final MKO time series consists of averages of 5 consecutive data points (covering about 5 min each). To compensate for the dependency of the pulsation amplitude on the used filter we scaled the Strömgren y time series with a heuristically determined factor of 0.8 (the average ratio between the strongest amplitudes in the y and V filter time series) before combining them with the Johnson V data of the other sites. The combined light curves of V588 Mon and V589 Mon are given in Fig. 2.

4. Global stellar parameters

We used our own Strömgren photometry as well as published Geneva and JHK photometry and applied photometric calibrations to estimate the physical parameters. In addition, we used spectroscopic observations to obtain radial velocities and $v \sin i$.

4.1. Photometric calibrations

Using the Strömgren photometry carried out at OSN, we were able to refine the photometric indices ($b-y$, m_1 and c_1) given by Peña et al. (2001) and others. They are listed in Table 2 (where β refers to values from Peña et al. 2001) and serve as input for the routine TempLoggG (Kaiser 2006), which determines effective temperature, $T_{\rm eff}$, surface gravity, $\log g$, absolute magnitude, M_V, and reddening, $E(b-y)$, based on calibrations described by Moon & Dworetsky (1985) and Napiwotzki et al. (1993). The luminosity, $L/L_\odot$, can be estimated from the absolute bolometric magnitude, $M_{\rm bol}$, which is obtained from the visual magnitude, V, and the bolometric correction, BC_V. Interpolation in the theoretical tables of Lejeune & Schaerer (2001) leads to BC_V of 0.1 and 0.125 for V588 Mon and V589 Mon, respectively.

In our next step, we used the Geneva 7 color photometry (accessible via the WEBDA[2] database) and a calibration described by Künzli et al. (1997), which uses the indices d and $B2-V1$ to estimate effective temperatures and surface gravities. Finally, infrared colors from the 2MASS catalog (Curti et al. 2003) are used to calibrate effective temperatures (Masana et al. 2006). The authors also provide a calibration for the bolometric correction of K magnitudes leading to a BC_K of 0.51 and 0.88 for V588 Mon and V589 Mon, respectively. From this we obtain absolute bolometric magnitudes and luminosities.

A summary of global stellar parameters based on different photometric calibrations is given in Table 2. We note that the errors (given in parentheses) are formal errors based on the uncertainties of the observations only. They do not reflect the uncertainty of the calibration itself. For example, according to Kaiser (2006), the typical error of the Strömgren temperature calibration is about 5%, corresponding to roughly 350 K for the temperature range under consideration. This is also reflected by the fact that values of fundamental parameters based on independent calibrations can differ significantly. Sometimes, the error ranges do not even overlap. On the other hand, Masana et al. (2006) found the error of their temperature calibration for FGK stars based on 2MASS photometry to be less than 1% (75 and 68 K in our case). We therefore assume the effective temperatures based on the 2MASS photometry to be the most reliable ones. This is also supported by the fact that the thus obtained temperatures correspond to a A7 III and a F1 III star (Gray 1992) which is in good agreement with spectral types (A7 III-IV and F1.5 III) provided by the Tycho–2 Spectral Type Catalog (Wright et al. 2003). For consistency reasons we also prefer the 2MASS values for the bolometric magnitude and luminosity but note that for both stars values independently derived from the cluster distance are within the uncertainties.

Figure 3 shows the uncertainty box for both stars in the HR-Diagram along with PMS evolutionary tracks for various masses. The latter were computed with the Yale Rotating

[2] http://www.univie.ac.at/webda/

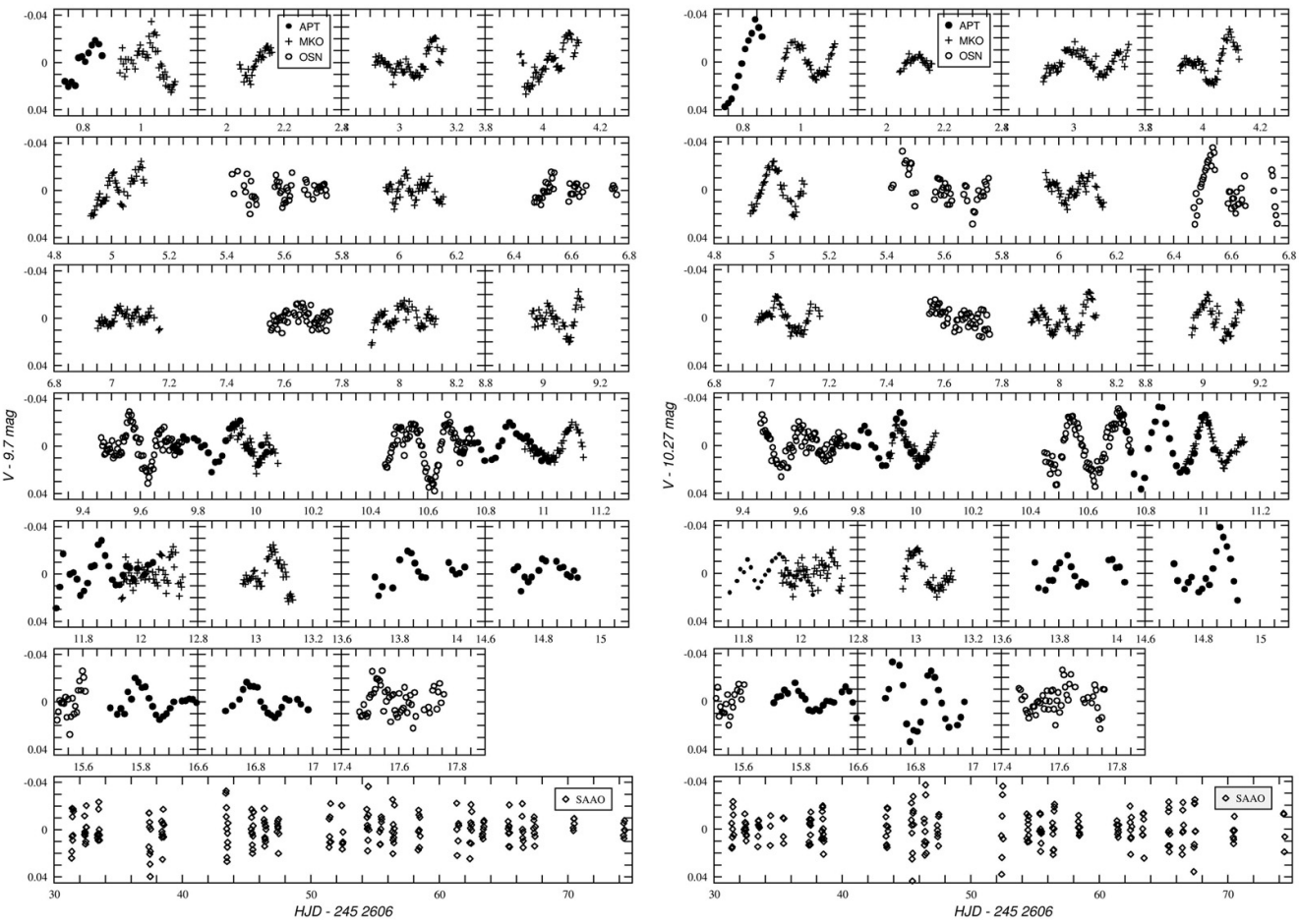

Fig. 2. Differential multisite photometry of V588 Mon (*left panel*) and V589 Mon (*right panel*): APT (filled circles), MKO (plus signs), OSN (open circles), and SAAO (open diamonds) observations.

Table 2. Our Strömgren color indices (β refers to values from Peña et al. 2002) and a summary of fundamental parameters. Values for absolute bolometric magnitude, $T_{\rm eff}$, $\log g$ and $\log L/L_\odot$ derived from Strömgren (Str), Geneva (Gen) and 2MASS (2M) photometry or the cluster distance (CD). Formal last digits errors are given in parentheses and the most reliable values are bold.

	V	$b-y$	m_1	c_1	β	$E(b-y)$	$M_{\rm bol}$	$T_{\rm eff}$	$\log g$	$\log L/L_\odot$	source
V588	9.720(10)	0.146(07)	0.169(08)	1.010(15)	2.804(20)	0.010	0.57(34)	7740(120)	3.6(3)	1.66(14)	Str
							–	7300(100)	3.8(2)	–	Gen
							0.17(25)	7450(150)	–	1.83(10)	2M
							0.42(26)	–	-	1.73(10)	CD
V589	10.301(27)	0.261(10)	0.192(11)	0.744(22)	2.709(10)	0.033	1.67(36)	6980(80)	3.6(3)	1.24(15)	Str
							–	6400(80)	3.0(3)	–	Gen
							0.79(25)	6800(100)	–	1.58(10)	2M
							1.03(26)	–	–	1.49(10)	CD

Evolutionary Code (YREC, Guenther et al. 1992) with an initial hydrogen and metal mass fraction of $(X, Z) = (0.71, 0.019)$ and a standard mixing length parameter $\alpha = 1.8$. Furthermore, the edges of the δ Scuti instability strip (which coincide well with the boundaries of the pulsating PMS star strip, Zwintz 2008) as well as the ZAMS (Pamyatnykh, private communication) and the Palla & Stahler (1993) birthline are indicated by dashed lines.

4.2. Spectroscopic observations

On Oct, 4th 2003, single spectra were obtained using the COUDE Spectrograph mounted on the 2m RCC Telescope at NAO Rozhen (Bulgaria). The spectra range from about 5750 to 5950 Å with a spectral resolution of ~15 000 and a signal-to-noise ratio of roughly 70 and 60 for V588 Mon and V589 Mon, respectively. The reduced and normalized spectra are illustrated as grey lines in the top and middle panel of Fig. 4. Black lines correspond to synthetic spectra folded with the instrumental profile and broadened with a projected rotational velocity $v\sin i$ of 130 ± 20 and 60 ± 10 km s^{-1} for V588 Mon (labeled with a) and V589 Mon (labeled with b), respectively. From the wavelength shift between observed and synthetic spectrum we obtained a radial velocity of 10 ± 10 km s^{-1} for V588 Mon and 30 ± 5 km s^{-1} for V589 Mon.

In a first step, synthetic spectra were computed using Atc (Stütz et al. 2006) and SYNTH3 (Piskunov 1992) with effective

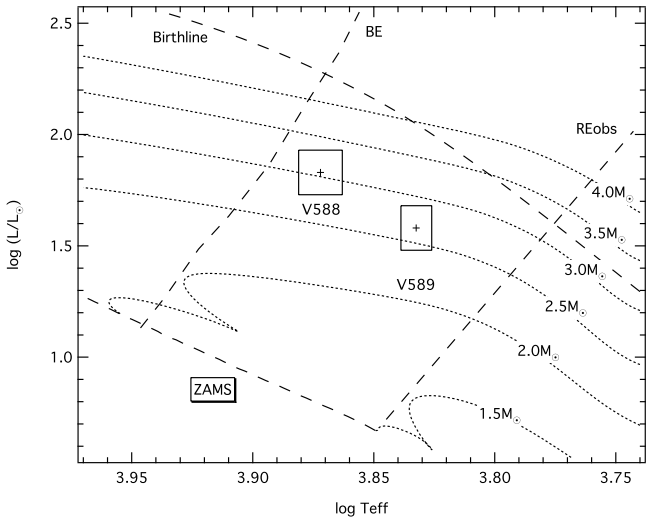

Fig. 3. Theoretical HR-Diagram showing the uncertainty box location of V588 Mon and V589 Mon and PMS evolutionary tracks computed using YREC (Guenther et al. 1992).

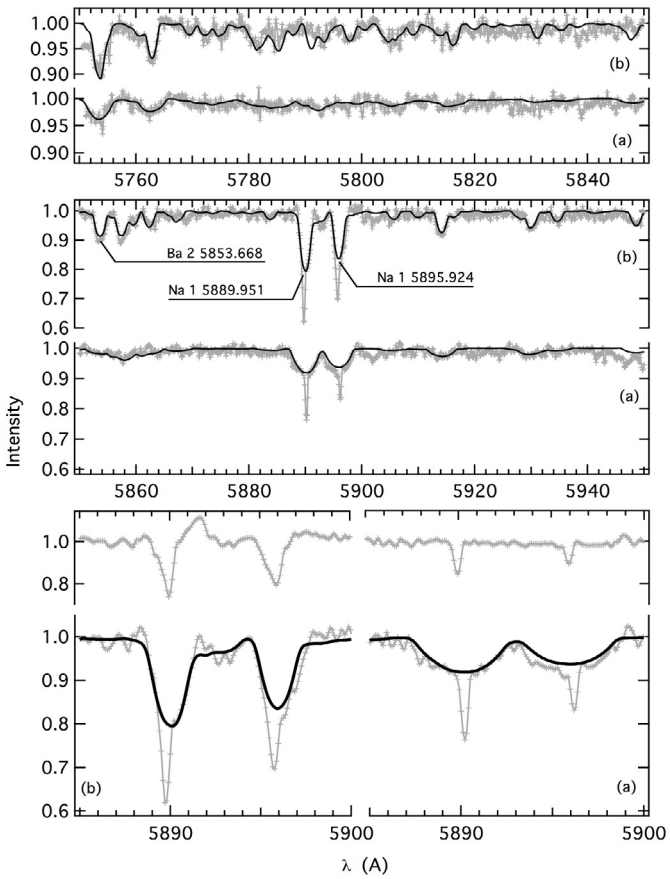

Fig. 4. A comparison between spectrum synthesis calculations (black lines) and observed spectra (grey lines) of V588 Mon **a)** and V589 Mon **b)** is shown in *the top and middle panel*. The lower part of the bottom panel illustrates blow-ups centered on the Na I D doublet. The upper part shows the difference between the observed and synthetic spectra hence the *non-stellar* component of these spectral lines.

temperatures and surface gravities as listed in Table 2 and solar abundance (Asplund et al. 2005). Compared to the observations, both synthetic spectra show Na I D features that are too weak (for V589 Mon also the Ba II line is too weak). This could either be due to over-abundant Na (and Ba for V589 Mon) or due to wrong effective temperatures or, even more likely, due to wrong surface gravities. To check this, we varied the temperature and surface gravity in Table 2 given errors, but found the corresponding changes in the line depths not enough to fit the observations. Hence, either the abundances are wrong or the real fundamental parameters lie outside the photometrically determined boundaries. However, since the present spectra do not include enough spectral lines there is no way to disentangle these effects. We therefore simply changed the Na abundance from −5.87 to −5.5 (and Ba from −9.91 to −9.0 for V589 Mon) and repeated the spectral synthesis to fit the observed spectra.

The lower part of the bottom panel in Fig. 4 shows blow-ups centered on the Na I D doublet illustrating that the spectral lines consist of two components. A stellar component broadened by rotation and a narrow component produced by interstellar gas absorption along the line of sight. Residuals after subtraction of the synthetic spectra from the observed ones are given in the upper part of the lower panel in Fig. 4 and show the non-stellar component only. The residual Na I D features for both stars have similar radial velocities (23 ± 5 and 18 ± 5 km s^{-1}), which are in agreement with the average radial velocity of the cluster. Furthermore, we found the ratios of the residual line depths of the Na I D_1 and D_2 lines between spectrum (a) and (b) to be about 1.7. This corresponds to the intensity ratio of V588 Mon and V589 Mon of ∼1.71 derived from the difference of the Johnson V magnitudes. Hence, the Na I column density along the line of sight is similar for both stars.

We conclude that the presence of interstellar gas absorption in both observed spectra most likely excludes the possibility of both stars being foreground stars (as suggested by Peña et al. 2001 based on their distance determination). Due to the similar Na column densities it appears to be very unlikely that one star is a cluster member while the other is a background star. Either both stars are members of the cluster or both stars are background stars.

5. Frequency analysis

We used the routine SigSpec (Reegen 2007) to identify significant frequencies in the discrete Fourier transform (DFT, Deeming 1975) spectra of both data sets. SigSpec employs an exact analytical solution for the probability that a peak of given amplitude could be generated by white noise. Its main advantage over commonly used signal-to-noise ratio estimates is that SigSpec appropriately incorporates the frequency and phase angle in Fourier space as well as the time domain sampling, hence using all available information instead of amplitude only. The SigSpec spectral significance is defined as the logarithm of the inverse false-alarm probability that a DFT peak of a given amplitude arise from noise in a non-equidistantly spaced data set. On average, a signal-to-noise ratio of 4, suggested as a reliable significance estimator by Breger et al. (1993), roughly corresponds to a SigSpec significance value of 5.46. The SigSpec significance is equal to $\log_{10}$ the probability that the peak is not due to white noise. In other words, a signal amplitude of 4 times the noise level would appear by chance at its given frequency in only one of $10^{5.46}$ cases, assuming white noise. SigSpec automatically identifies the peak with the largest significance in the frequency range searched, determines the amplitude and phase associated with this frequency through least-squares sinusoidal fitting, and subtracts that signal from the time series. The residuals are then used in the next SigSpec significance calculation, and the process is repeated until there is no frequency remaining

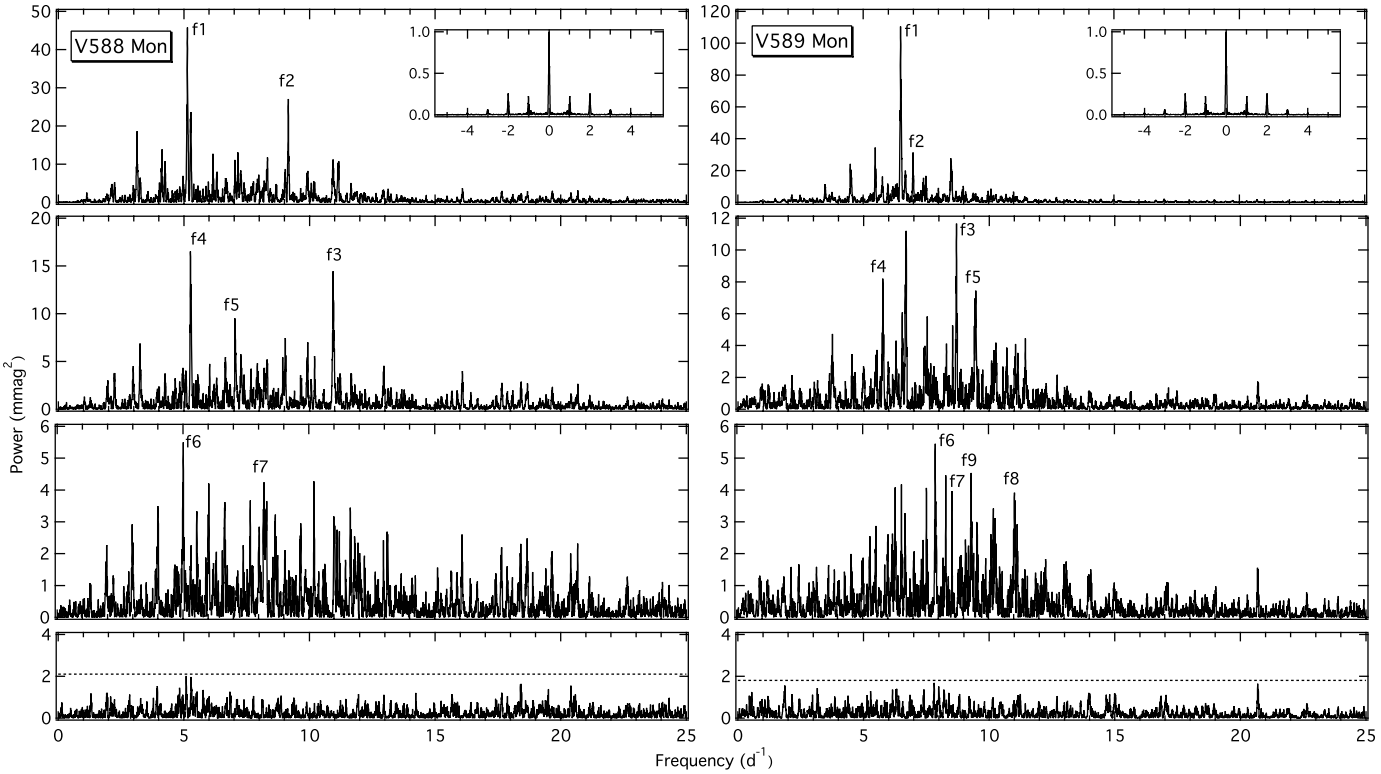

Fig. 5. Fourier power spectra of V588 Mon and V589 Mon for the multisite photometry. The numbering scheme of the peaks refers to the frequencies listed in Table 3 and are limited (for better visibility) to frequencies with sig > 10. *The bottom panels* correspond to power spectra of residual time series after prewhitening all significant frequencies. The dashed lines correspond to the significance limit of 5.46. Spectral window functions are shown in insets.

with SigSpec significance above the threshold value set for the search.

We find 16 and 20 frequencies in the combined Johnson V photometry of V588 Mon and V589 Mon, respectively, with a SigSpec significance greater than 5.46 (equivalent to $S/N \sim 4$) from 0–30 d^{-1} and we list them in Table 3. The frequency uncertainties are determined according to Kallinger et al. (2008), who define an upper limit for the frequency and relative amplitude error of a least-squares sinusoidal fit as $(T \cdot \sqrt{sig})^{-1}$ and $(1/\sqrt{sig})$, respectively, where T corresponds to the data set length. A multisine fit of the strongest amplitude frequencies to the Johnson B (APT and SAAO) and Strömgren *ubvy* (OSN) time series result in the amplitudes given in Tables 3 and 4.

Figure 5 illustrates sequences of Fourier power spectra during the prewithening procedure from the original combined data (top) to the residual time series after subtracting all significant signal (bottom). Dashed lines in the bottom panels indicate the detection limits (SigSpec significance equal to 5.46) of roughly 1.4 and 1.25 millimagnitudes for the V588 Mon and V589 Mon times series, respectively. The average amplitudes in the residual amplitude spectra are about 395 and 340 ppm, slightly larger than one would expect from the detections limits (about 350 and 310 ppm), indicating that there is still some unidentified signal left.

5.1. V588 Mon

In a first step we searched for linear combinations among the identified frequencies. The presence of linear combinations in δ Scuti-type stars is a well-known phenomenon (e.g. Breger et al. 2005). This is most likely due to the fact that the intrinsic signals slightly differ from ideal harmonic oscillations. Co-adding such signals enforces linear combination in the Fourier domain. From the 16 frequencies considered to be significant and ranging from ~6.8–1.4 mmag, we identiy f15 as the difference of f11 and f10 (within 0.007 d^{-1}). Despite the fact that Peña et al. (2001) confirmed the variability found by Breger (1972) their frequency identification is questionable which is not surprisingly due to the poor spectral window. None of their listed three frequencies is reproduced by our analysis. Only their dominant frequency is close to a +2 d^{-1} alias peak of our dominant peaks f1 at about 5.13 d^{-1}.

5.2. V589 Mon

Among the 20 significant frequencies ranging from ~10.7–1.2 mmag, we identifiy f20 as a linear combination of f7 and f11 (within 0.005 d^{-1}) and f12 as an alias peak of f2 (within 0.006 d^{-1}), respectively. Similar to V588 Mon, our frequency analysis is not consistent with the frequencies found by Peña et al. (2001). Again, only their dominant peak can be interpreted as an +1 d^{-1} alias of our dominant frequency at about 6.48 d^{-1}.

6. A first analysis

Although the main objective of this work is to refine the multi–periodicity of V588 Mon and V589 Mon and to confirm their cluster membership and consequently their evolutionary status, we are curious about the nature of the detected frequencies. We therefore use the period – mean density relation for pulsating stars to perform a first asteroseismic analysis. This relation can

Table 3. Oscillation frequencies of V588 Mon and V589 Mon. Last digits errors (given in parentheses) are calculated according to Kallinger et al. (2008).

	Frequency (d^{-1})	sig	V (mmag)	B
V588 Mon				
f6	5.0121(37)	13.3	2.40(66)	
f15 = f11-f10	5.0951(53)	6.6	1.40(54)	
f1	5.1383(18)	56.2	6.77(90)	8.12(62)
f4	5.2586(25)	28.7	3.99(74)	4.49(58)
f9	5.5464(46)	8.7	1.77(60)	
f5	7.0281(30)	20.3	3.03(67)	2.87(63)
f12	7.6742(48)	8.1	1.58(55)	
f7	8.2171(40)	11.5	2.13(63)	
f13	8.3079(50)	7.2	1.65(61)	
f2	9.1579(21)	42.4	5.27(81)	5.37(59)
f3	10.9374(24)	31.5	3.98(71)	4.24(61)
f10	10.9917(47)	8.4	1.77(61)	
f8	11.6478(45)	8.9	1.87(63)	
f14	11.8379(52)	6.8	1.47(56)	
f16	13.1324(54)	6.3	1.41(56)	
f11	16.0861(47)	8.2	1.71(60)	
V589 Mon				
f20 = f7-f11	1.8691(57)	5.7	1.25(52)	
f15	5.0175(55)	6.0	1.32(54)	
f4	5.7636(29)	21.4	3.12(67)	5.41(80)
f12 = f2-1d^{-1}	5.9920(46)	8.7	1.65(56)	
f19	6.2900(56)	5.8	1.25(52)	
f1	6.4885(13)	109.7	10.68(99)	15.69(86)
f11	6.6792(45)	9.1	1.72(57)	
f2	6.9861(17)	67.4	6.62(81)	12.33(84)
f16	7.8124(56)	5.9	1.29(53)	
f6	7.8821(37)	13.6	2.35(63)	0.54(86)
f17	8.3105(56)	5.9	1.22(50)	
f7	8.5438(39)	12.3	2.09(60)	
f3	8.6975(28)	24.0	3.45(70)	5.87(82)
f14	9.0827(49)	7.7	1.53(55)	
f9	9.3092(41)	11.0	2.03(61)	
f5	9.4657(37)	13.7	2.39(65)	1.22(82)
f10	10.1926(45)	9.2	1.75(58)	
f13	10.2597(49)	7.8	1.53(55)	
f8	11.0484(39)	12.1	2.05(59)	
f18	11.1723(56)	5.9	1.19(49)	

Table 4. Strömgren *uvby* amplitudes of the highest amplitude frequencies as listed in Table 3.

	f (d^{-1})	u	v	b	y
		(mmag)			
V588 Mon					
f1	5.1383	10.0(14)	10.9(09)	9.6(08)	6.9(09)
f2	9.1579	6.6(15)	7.6(10)	6.7(07)	5.8(09)
f3	10.9374	6.3(15)	8.0(09)	7.1(07)	6.0(08)
f4	5.2586	2.9(15)	6.0(09)	5.2(07)	5.1(09)
f5	7.0281	6.4(15)	7.1(08)	6.2(07)	5.4(08)
V589 Mon					
f1	6.4885	18.9(20)	21.0(10)	16.9(09)	12.2(09)
f2	6.9861	14.0(22)	16.3(11)	12.4(10)	8.8(08)
f3	8.6975	4.4(18)	6.0(09)	5.5(08)	4.5(07)
f4	5.7636	4.6(20)	6.5(10)	5.2(08)	4.1(08)
f5	9.4657	5.2(17)	4.6(08)	3.8(07)	3.6(08)

also be written as a period – luminosity – color – mass relation of the form (Breger & Pamyatnykh 1998):

$$\log P = -0.3 M_{\rm bol} - 3 \log T_{\rm eff} - 0.5 \log M + \log Q + 12.708 \quad (1)$$

where P and M are the period and stellar mass, respectively. For δ Scuti stars, a pulsation constant, Q, equal to 0.033 d corresponds to the radial fundamental period. For the first overtone Q is 0.025 d, for the second it is 0.02 d, and for the third 0.017 d. We now use $M_{\rm bol}$, $T_{\rm eff}$ from Table 2 and estimate the mass to be about $3.1 \pm 0.3\,M_\odot$ (see Fig. 3). Consequently we expect the radial fundamental frequency to be at 4.86 d^{-1} (or at least in the range of 4.33–5.45 d^{-1} when considering the errors for $M_{\rm bol}$, $T_{\rm eff}$, and M). Indeed, the largest amplitude frequency f1 falls into this range and is thus assumed to be the radial fundamental mode. The same can now be done for radial overtones. We estimate the first radial overtone to be in the range of 5.72–7.19 d^{-1}, the second harmonic in the range of 7.15–9.0 d^{-1}, and the third between 8.41 and 10.58 d^{-1}.

From Fig. 3, we estimated a mass of $2.7 \pm 0.3\,M_\odot$ for V589 Mon and use $M_{\rm bol}$ and $T_{\rm eff}$ from Table 2 to evaluate the radial fundamental frequency to fall into the frequency interval between 4.7 and 5.97 d^{-1}. The first, second, and third overtones are determined to be in the range of 6.2–7.86 d^{-1}, 7.75–9.84 d^{-1}, and 9.12–11.58 d^{-1}, respectively.

Although there seems to be a surprisingly good agreement between some of the observed frequencies and theoretically determined fundamental modes (and overtones) we note that no reliable mode identification can be done because nearly all detected frequencies fall into one of the listed frequency ranges. Nevertheless, there are more significant frequencies present than one can expect for a sequence of radial modes. We interpret this as an indication for the presence of nonradial modes.

7. Other variable stars

Among the 34 stars observed at MKO, in addition we found two other variable stars were found. Star 4 (NGC 2264 1 or GSC 00750-01459) shows variability with a period of about 0.38d and an amplitude of about 0.1 mag in Johnson V. The origin of the variability is suspected to be an eclipsing binary or at least two surface spots. This is illustrated in the phase plot (top panel of Fig. 6). Star 5 (NGC 2264 RMS 559) is variable with a period of 0.51d and an amplitude of ~0.2 mag. A phase plot (bottom panel of Fig. 6) more clearly shows that the variability is caused by an eclipsing companion.

8. Conclusions

Some 35 years ago, Breger (1972) established a new class of variable stars, the pulsating PMS stars, on the basis of his findings in V588 Mon and V589 Mon. This claim was mainly built on the assumption that both stars are members of the young open cluster NGC 2264 and therefore could not be old evolved δ Scuti stars. For many years, other pulsating PMS stars were detected but the membership of the two "prototypes" was never verified. It was even questioned by Peña et al. (2002). Based on a detailed analysis of many different sources of observations, including our

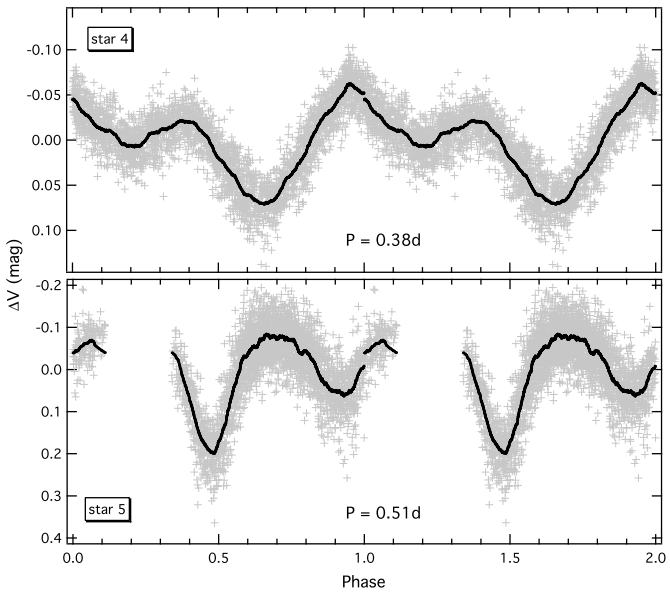

Fig. 6. MKO data of star 4 and 5 phased with their dominant periods. Plus symbols correspond to the original data and black lines indicate a running average.

own high-precision time series photometry, we found strong evidence that both stars are members of NGC 2264 and hence are indeed in their PMS evolutionary phase.

We have also confirmed that both stars are variable. We have performed a detailed frequency analysis resulting in well-populated eigenspectra and we have deduced the most feasible fundamental parameters. By using the period – mean density relation for classical pulsators, we find that both stars show variability in a frequency range where it is expected for stars in the δ Scuti instability region. We also draw first conclusions on which of the detected frequencies are consistent with the fundamental radial mode (and its overtones). But the still quite large uncertainties of the fundamental parameters prevent us from performing a reliable mode identification. The presence of more significant frequencies than one would expect for a sequence of radial modes lets us assume that both stars also show nonradial pulsation. However, we found no characteristic frequency spacing indicating a large frequency separation or rotational splittings.

Finally, we want to mention that the two stars were proposed to the MOST Science Team for observations as the PMS stars with the richest frequency spectrum so far. And indeed, high-precision space-photometry was obtained for V588 Mon and V589 Mon, which will be the topic of a follow-up paper along with a detailed model analysis. We also want to emphasize that better spectroscopic observations, with higher spectral resolution and S/N, are needed to constrain more accurate fundamental parameters. But this is also in progress.

Acknowledgements. We kindly thank I. Iliev (NAO Rozhen, Bulgaria) for obtaining and reducing the spectra and Richard Crowe (University of Hawaii) for giving us access to the (normally non-public) 22inch telescope of the University of Hawaii. The OSN observations were kindly supported by Rafael Garrido Haba and Eloy Rodriguez and the SAAO measurements were obtained by Peter Martinez. T.K. W.W.W. are supported by the Austrian Research Promotion Agency (FFG), and the Austrian Science Fund (FWF P17580) and K.Z. acknowledges funding from the Austrian Science Fund (FWF, project T335-N16).

References

Asplund, M., Grevesse, & N., Sauval, A. J., Cosmic Abundances as Records of Stellar Evolution and Nucleosynthesis in honor of David L. Lambert, ASP Conference Series, Vol. 336, Proceedings of a symposium held 17–19 June, 2004 in Austin, Texas, Ed. T. G. Barnes III & F. N. Bash (San Francisco: ASPC), 2005, p. 25
Breger, M. 1972, ApJ, 171, 539
Breger, M., & Pamyatnkh, A. 1998, A&A, 332, 958
Breger M., Stich J., Garrido R., Martin B., et al. 1993, A&A, 271, 482
Breger, M., Lenz, P., Antoci, V., et al. 2005, A&A, 435, 955
Curti, R. M., Skrutskie, M. F., van Dyk, S., et al. 2003, `http://www.ipac.caltech.edu/2mass/releases/allsky/ doc/explsup.html`
Deeming, T. J. 1975, Ap&SS, 36, 137
Guenther, D. B., Demarque, P., Kim, Y.-C., & Pinsonneault, M. H. 1992, ApJ, 387, 372
Guenther, D. B., Kallinger, T., Zwintz, K., et al. 2007, ApJ, in press
Gray, D. F. 1992, The observation and analysis of stellar photospheres (Cambridge University Press)
Hog, E., Fabricius, C., Makarov, V. V., et al 2000, A&A, 355, L27
Kallinger T. 2005, CoAst, 146, 45
Kallinger, T., Reegen, P., & Weiss, W. W. 2008, A&A, 481, 571
Kaiser, A 2006, in Astrophysics of Variable Stars, ed. by Sterken, C., & Aerts, C. ASP Conf. Series, 349, 257
Künzli, M., North, P., Kurucz, R. L., & Nicolet, B. 1997, A&ASS, 122, 51
Kurtz, D., & Marang, F. 1995, MNRAS, 276, 191
Lamm, M. H., Bailer-Jones C. A. L., Mundt, R., et al. 2004, A&A, 417, 557
Lejeune, T., & Schaerer, D. 2001, A&A, 366, 538
Marconi, M., Ripepi, V., Alcalá, J. M., et al. 2000, A&A, 355, L35
Masana, E., Jordi, C., & Ribas, I. 2006, A&A, 450, 735
Moon, T. T., & Dworetsky, M. M. 1985, MNRAS, 217, 305
Napiwotzki, R., Schoenberner, D., & Wenske, V. 1993, A&A, 268, 653
Palla, F., & Stahler, S. W. 1993, ApJ, 418, 414
Peña J. H., Peniche R., Cervantes F., & Parrao L. 2002, RMxAA, 38, 31
Pérez, M. R., Thé, P. S., & Westerlund, B. E. 1987, PASP, 99, 1050
Piskunov, N. 1992, Stellar Magnetism – Proceedings of the international meeting on the problem Physics and Evolution of Stars, ed. Yu. V. Glagolevskij & I. I. Romanyuk, St. Petersburg, 92
Rebull, L. M., Makidon, R. B., Strom, S. E., et al. 2002, AJ, 123, 1528
Reegen P. 2007, A&A, 467, 1353
Strom, K. M., Strom, S. E., & Yost, J. 1971, ApJ, 165, 479
Stütz, Ch., Bagnulo, S., Jehin, E., et al. 2006, A&A, 451, 285
Sung, H., Bessell, M. S., & Lee, S.-W. 1997, AJ, 114, 6
Suran, M., Goupil, M., Baglin, A., et al. 2001, A&A, 372, 233
Valenti J.A., Piskunov N. & Johns-Krull C.M. 1998, ApJ, 498, 851
Wolf, M. 1924, A.N., 221, 379
Wright, C. O., Egan, M. P., Kraemer, K. E., & Price, S. D. 2003, AJ, 125, 359
Zwintz, K. 2008, ApJ, 673, 1088
Zwintz, K., & Weiss, W. W. 2006, A&A, 457, 237
Zwintz, K., Marconi, M., Reegen, P., et al. 2005, MNRAS, 357, 345